JOC*Note*

Absolute Configuration of Myrobotinol, New Fused-Hexacyclic Alkaloid Skeleton from *Myrioneuron nutans*

Van Cuong Pham,*[,†,§] Akino Jossang,[†] Thierry Sévenet,[‡] Van Hung Nguyen,[§] and Bernard Bodo*[,†]

Laboratoire de Chimie et Biochimie des Substances Naturelles-CNRS, Muséum National d'Histoire Naturelle, 63 rue Buffon, 75005 Paris, France, Institut de Chimie des Substances Naturelles, CNRS-91198 Gif-sur-Yvette cedex, France, and Institute of Chemistry−Vietnamese Academy of Science and Technology, 18 Hoang Quoc Viet road, Hanoi, Vietnam

bodo@mnhn.fr; phamvc@ich.vast.ac.vn

Received August 9, 2007

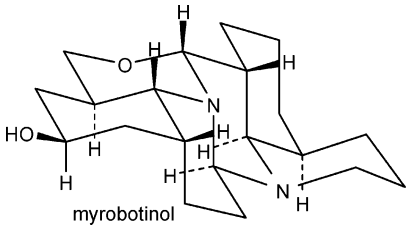

Myrobotinol (**1**) was isolated from the leaves of *Myrioneuron nutans* (Rubiaceae) and its structure determined from spectral data, including mass spectrometry and 2D NMR. This compound presents a new hexacyclic alkaloid skeleton including a 1,3-oxazine and aminal functionality. The absolute configuration of myrobotinol was established by using Mosher's method. A plausible biosynthetic pathway starting from L-lysine via Δ-piperideine was proposed for this hexacyclic alkaloid.

The genus *Myrioneuron* produces a group of polyheterocyclic alkaloids and we have previously reported the structural elucidation and the total synthesis of several tricyclic alkaloids from *M. nutans*.[1a−c] These compounds have various alkaloid skeletons which all contain a *cis*-decahydroquinoline (*cis*-DHQ) moiety and for some of them, an oxazine motif. In continuation of our research of alkaloids from this plant, further purification of the crude alkaloid fraction has led to the isolation of a new hexacyclic alkaloid skeleton, which we designate as myrobotinol (**1**). Its absolute configuration was determined by Mosher's method taking advantage of the presence of a secondary alcohol function. Finally, a plausible biosynthetic pathway is described for myrobotinol (**1**) by condensation of two *cis*-DHQ derivatives, biogenetically derived from L-lysine.[2a,b]

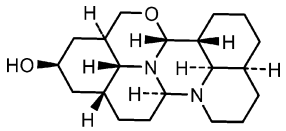

The crude alkaloid fraction (29.5 g) obtained from the dry leaves of *M. nutans* (5.5 kg) was purified by repeated open column chromatography over silica gel eluted with CH_2Cl_2/MeOH gradient to afford myrobotinol (**1**, 20 mg).

Myrobotinol (**1**) was obtained as an optically active colorless crystalline solid, mp 225−226 °C, $[\alpha]^{20}_D$ +36.4 (*c* 0.4, MeOH). In its ESI-MS, the protonated molecular ion $[M + H]^+$ was observed at *m*/*z* 333.2538 (calcd 333.2542 for $C_{20}H_{33}N_2O_2$), in agreement with the molecular formula $C_{20}H_{32}N_2O_2$. The 1D NMR (^1H and ^{13}C) spectra revealed nine sp^3 methine and eleven methylene groups. The six degrees of unsaturation were thus assigned to six rings. $^1H-^1H$ COSY data allowed the determination of two sets of connections as indicated by bold bonds in Figure 1. The **A**-fragment was defined through a set of correlations extending from CH_2-2 (δ_H 2.66 and 2.76) through H-11 (δ_H 4.13) observed in the COSY 45 and TOCSY spectra. In addition, H-10 (δ_H 3.11) was correlated to both H-5 (δ_H 1.92) and H-9 (δ_H 2.24). Similarly, the **B**-fragment was determined by correlations starting from CH_2-13 (δ_H 3.25 and 3.98) to H-21 (δ_H 4.19) together with those of H-23 (δ_H 2.69) with H-14 (δ_H 2.15) and H-18 (δ_H 1.93). The chemical shifts of CH_2-2 (δ_C 38.0, δ_H 2.66 and 2.76), CH-10 (δ_C 57.4, δ_H 3.11), and CH-23 (δ_C 64.5, δ_H 2.69) suggested they were attached to a nitrogen and those of CH-11 (δ_C 91.6, δ_H 4.13) were characteristic of a methine linked to both a nitrogen and an oxygen. In the HMBC spectrum, the correlations of H-10 with C-2 and C-21 indicated direct linkage of N-1 with C-2, C-10, and C-21. Furthermore, H-11 was correlated to C-13, C-21, and C-23, this latter carbon being further correlated to H-21 and CH_2-13. From these data, N-22 was linked to CH-11, CH-21, and CH-23 and in addition both CH-11 and CH_2-13 were bonded to O-12. The planar structure of myrobotinol (**1**) was thus elucidated as drawn in Figure 1.

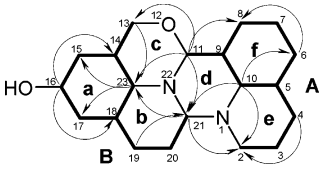

FIGURE 1. $^1H-^1H$ COSY (—) and HMBC (→) correlations for **1.**

The relative configuration of myrobotinol (**1**) was established by analysis of $^1H-^1H$ coupling constants and NOE interactions. Hence, the H-16 proton had two *trans*-diaxial ($J_1 = J_2 = 11.3$ Hz) and two *gauche* ($J_3 = J_4 = 4.5$ Hz) coupling constants indicating its axial disposition on the **a**-ring. The five protons

† Muséum National d'Histoire Naturelle.
‡ Institut de Chimie des Substances Naturelles.
§ Institute of Chemistry−Vietnamese Academy of Science and Technology.

(1) (a) Pham, V. C.; Jossang, A.; Chiaroni, A.; Sévenet, T.; Bodo, B. *Tetrahedron Lett.* **2002**, *43*, 7565−7568. (b) Pham, V. C.; Jossang, A.; Chiaroni, A.; Sévenet, T.; Nguyen, V. H.; Bodo, B. *Org. Lett.* **2007**, *9*, 3531. (c) Pham, V. C.; Jossang, A.; Sévenet, T.; Nguyen, V. H.; Bodo, B. *Tetrahedron* **2007**, *63*, 11244.

(2) (a) Golebiewski, W. M.; Spenser, I. D. *J. Am. Chem. Soc.* **1984**, *106*, 7925. (b) Wanner, M. J.; Koomen, G. J. *Stud. Nat. Prod. Chem.* **1994**, *14*, 731.

10.1021/jo7017203 CCC: $37.00 © 2007 American Chemical Society
Published on Web 11/14/2007

TABLE 1. NMR Data for 1[a]

C no.	δ_C	δ_H m (*J*, Hz)	C no.	δ_C	δ_H m (*J*, Hz)
2	38.0	2.76 br dd (11.5, 4.6) 2.66 br dd (11.5, 11.3, 2.6)	13	73.0	3.98 dd (10.9, 4.6) 3.25 dd (10.9, 10.9)
3	25.9	1.71 m 1.49 m	14	26.6	2.15 ddddd (11.3, 11.3, 10.9, 4.6, 3.5)
4	24.0	1.53 m 1.27 m	15	37.0	1.68 m 0.79 ddd (11.3, 11.3, 11.3)
5	34.9	1.92 m	16	65.6	3.82 dddd (11.3, 11.3, 4.5, 4.5)
6	31.2	1.48 m 1.48 m	17	40.0	1.88 ddd (12.9, 4.5, 2.5) 1.45 m
7	20.1	1.38 m 1.38 m	18	36.1	1.93 m
8	27.4	1.40 m 1.32 m	19	25.3	1.61 m 1.51 m
9	30.6	2.24 dddd (11.9, 11.9, 3.5, 3.5)	20	30.0	1.65 m 1.65 m
10	57.4	3.11 dd (11.9, 4.8)	21	68.7	4.19 dd (9.3, 3.9)
11	91.6	4.13 d (3.5)	23	64.5	2.69 dd (11.3, 4.5)

[a] $CDCl_3$, 298 K; ^1H 400.13 MHz, ^{13}C 75.47 MHz.

to which H-14 was coupled were determined from the COSY spectrum as usual and four of them gave very well resolved and isolated signals from which it was easy to determine the reciprocal values of the coupling constants. These values were confirmed by the analysis of the aspect of the cross-peaks of the COSY and HSQC spectra, which in addition allowed the determination of the last coupling constant.[3] The H-14 proton presented five coupling constants: three large characteristic of *trans*-diaxial relationships ($J_1 = 11.3$ Hz, $J_2 = 11.3$ Hz, and $J_3 = 10.9$ Hz) and two *gauche* ($J_4 = 4.6$ Hz and $J_5 = 3.5$ Hz). This indicated that H-14 was axial on both the **a**- and **c**-rings and that it was in *trans*-diaxial relationship with H-23 which, in turn, appeared as a doublet of doublet with a *trans*-diaxial ($J_1 = 11.3$ Hz) disposition and a small ($J_2 = 4.5$ Hz) coupling constant: H-23 was thus in a gauche relationship with H-18. Furthermore, as the mutual coupling between H-11 and H-9 was small ($J = 3.5$ Hz) they were in a cis relationship. H-10 was in the *trans*-diaxial disposition with H-9 on both the **d**- and **f**-rings, as signified by their mutual coupling constant ($J = 11.9$ Hz). However, H-10 appeared as a double doublet ($J_1 = 11.9$, $J_2 = 4.8$ Hz) thus depicting its cis relationship with H-5. Finally, H-21 had a large ($J_1 = 9.3$ Hz) and a small ($J_2 = 3.9$ Hz) coupling constant and was thus axial on the **b**-ring. These results were confirmed from NOEs data obtained by a NOESY experiment: spatial interactions of H-23 with H-18, H-17_{ax}, H-15_{ax}, H-13_{ax}, and H-11, as well as those of H-21 with H-19_{ax}, H-14, and H-10, were observed (Figure 2). H-9 was also correlated with H-7_{ax}, H-4_{ax}, and H-2_{ax}. The correlations between H-10 and both H-14 and H-21 were presented. Finaly, H-16 was correlated with H-14. Complete analysis permitted establishing the relative configuration for myrobotinol (**1**) as 5*S**,9*R**,-10*R**,11*R**,14*R**,16*R**,18*R**,21*R**,23*R** (Figure 2), in which two *cis*-DHQ moieties substituted at C-8 were linked to each other via 1,3-oxazine and aminal functionality.

The absolute configuration of chiral secondary alcohols can be determined from NMR analysis of their derivatives with chiral auxiliary reagents such as methoxytrifluoromethylphenylacetic acid (MTPA) or methoxyphenylacetic acid (MPA).[4a−j] According to the former strategy, the absolute configuration of **1** was determined by Mosher's method, taking advantage of the presence of the secondary alcohol function at C-16. The

(3) Simova, S. *Magn. Reson. Chem.* **1998**, *36*, 505.

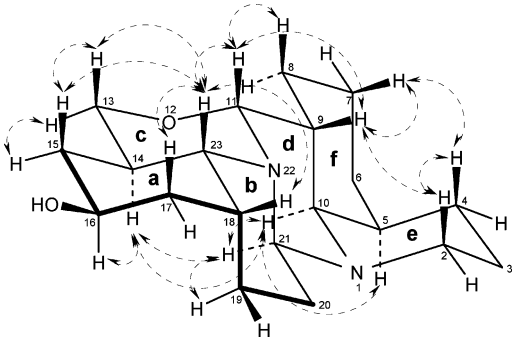

FIGURE 2. Selected NOE interactions for **1**.

(*R*)- and (*S*)-MTPA-myrobotinol esters **2** and **3** were prepared by esterification of myrobotinol (**1**) with (*R*)- and (*S*)-MTPA, respectively. The structures of the esters **2** and **3** were assigned by 2D NMR. The differences of proton chemical shifts between esters **2** and **3**, $\Delta\delta_{R-S}$ ($\delta_{(R)-\text{MTPA}-\text{myrobotinol}} - \delta_{(S)-\text{MTPA}-\text{myrobotinol}}$) were calculated (Figure 3). These values were positive on the up side of the molecule **1**, while they were negative on the other side. By using Mosher's model, the absolute configuration at the chiral carbon C-16 was thus determined as *R* (Figure 3). According to the relative configuration established above, the absolute configuration of myrobotinol (**1**) was defined as 5*S*,9*R*,-10*R*,11*R*,14*R*,16*R*,18*R*,21*R*,23*R*. This compound is a new alkaloid skeleton with six fused rings and named myrobotinol.

Retrosynthesis of myrobotinol (**1**) suggests that it could be biosynthesized from condensation of the two related *cis*-DHQ fragments **4** and **5**, followed by cyclization (Scheme 1). According to this hypothesis, the intermediates **4** and **5** resulting from L-lysine via Δ-piperideine[2a,b] are condensed to afford

(4) (a) Dale, J. A.; Dull, D. L.; Mosher, H. S. *J. Org. Chem.* **1969**, *34*, 2543. (b) Sullivan, G. R.; Dale, J. A.; Mosher, H. S. *J. Am. Chem. Soc.* **1973**, *38*, 2143. (c) Dale, J. A.; Mosher, H. S. *J. Am. Chem. Soc.* **1973**, *95*, 512. (d) Trost, B. M.; Belletire, J. L.; Godleski, S.; McDougal, P. G.; Balkovec, J. M. *J. Org. Chem.* **1986**, *51*, 2370. (e) Latypov, S. K.; Seco, J. M.; Quinoa, E.; Riguera, R. *J. Org. Chem.* **1996**, *61*, 8569. (f) Seco, J. M.; Latypov, S. K.; Quinoa, E.; Riguera, R. *J. Org. Chem.* **1997**, *62*, 7569. (g) Xiao, L.; Yamazaki, T.; Kitazume, T.; Yonezawa, T.; Sakamoto, Y.; Nogawa, K. *J. Fluorine Chem.* **1997**, *84*, 19. (h) Takahashi, H.; Iwashima, M.; Iguchi, K. *Tetrahedron Lett.* **1999**, *40*, 333. (i) Porto, S.; Durán, J.; Seco, J. M.; Quiñoá, E.; Riguera, R. *Org. Lett.* **2003**, *5*, 2979. (j) Zhang, Q. Y.; Carrera, G.; Gomes, M. J. S.; Aires-de-Sousa, A. *J. Org. Chem.* **2005**, *70*, 2120.

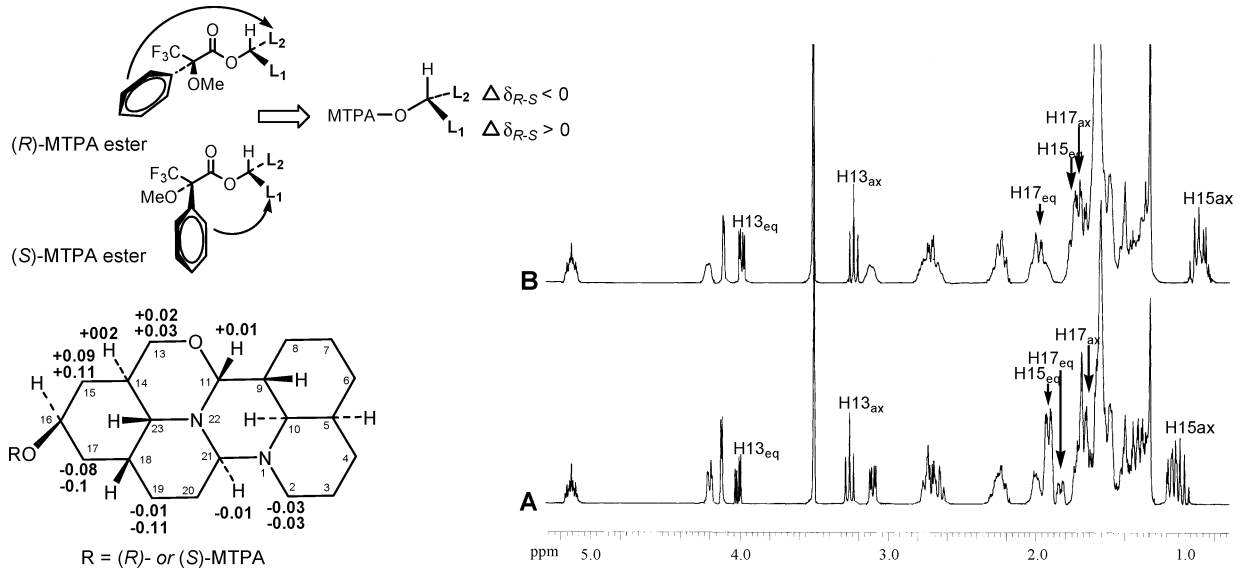

FIGURE 3. (A) ^{1}H NMR (400.13 MHz, $CDCl_3$, 298 K) of (*R*)-MTPA-myrobotinol (**2**); (B) ^{1}H NMR of (*S*)-MTPA-myrobotinol (**3**).

SCHEME 1. Proposed Biosynthetic Pathway for Myrobotinol (1)

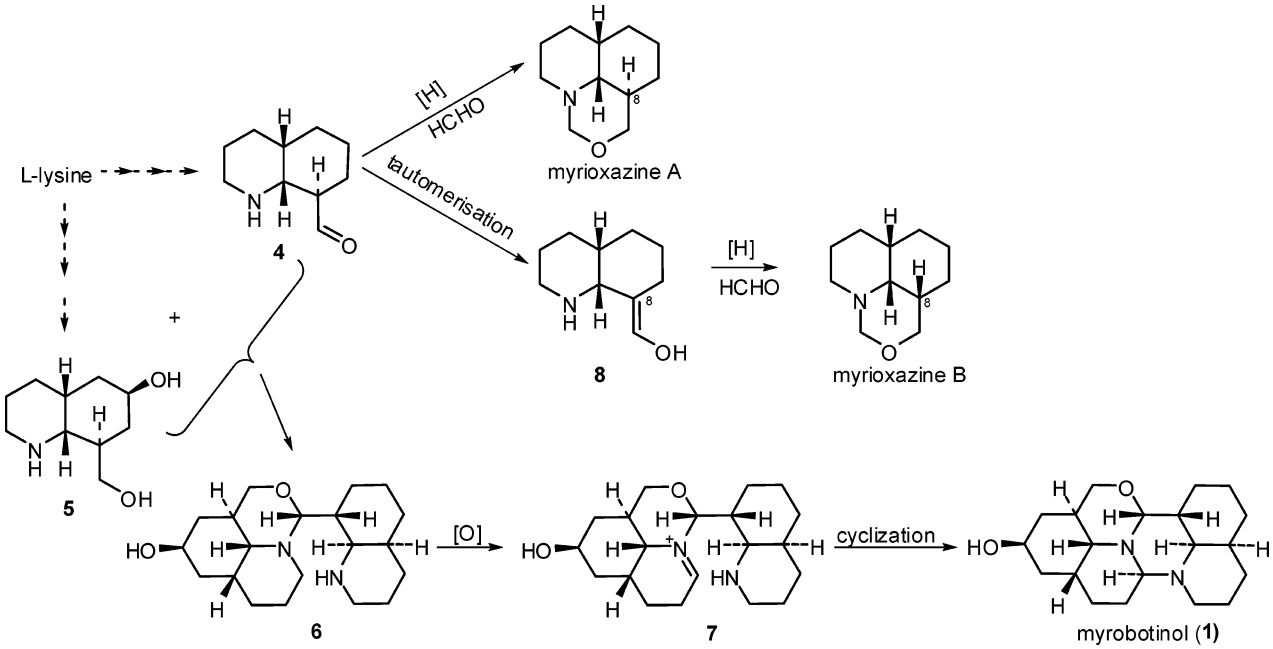

compound **6**. Oxidation of **6** provides the imine **7**, which is further cyclized to complete the biosynthesis of myrobotinol (**1**) (Scheme 1). The presence of myrioxazines A and B[1a] in the plant *M. nutans* provides support for the hypothetical biosynthetic pathway shown in Scheme 1 for myrobotinol (**1**).

Cytotoxic and antiplasmodial activities of myrobotinol (**1**) were evaluated on KB cell lines and on *Plasmodium falciparum* (FcB1 strain), respectively. Myrobotinol (**1**) was found to be inactive in two cases (IC_{50}: >33 μg/mL on KB and 20 μg/mL (56 μM) on *P. falciparum*). However, its MTPA derivatives **2** and **3** showed significant activity on KB cell lines and on *P. falciparum*. For cytotoxicity on KB cell, **2** and **3** displayed an IC_{50} of 2 μg/mL (4.5 μM) and 3 μg/mL (6 μM), respectively, while these values were 2 μg/mL (4.5 μM) for both **2** and **3** when evaluated on *P. falciparum*. This observation suggested that the antiplasmodial activity of **2** and **3** could be due to their cytotoxicity.

In summary, myrobotinol (**1**), a novel alkaloid with an unprecedented fused-hexacyclic skeleton, was isolated from *M. nutans*. The absolute configuration of **1** was established by using Mosher's method. For understanding of the bioformation of myrobotinol (**1**) in the plant, a plausible biosynthetic pathway was proposed.

Experimental Section

Plant Material and Extraction. *M. nutans* Drake was collected in North Vietnam in June 2000 and a specimen (VN 700) was deposited in the Institute of Botany-VAST-Vietnam. The dried and ground leaves (5 kg) were alkalinized with aqueous NH_4OH (10%) and extracted with CH_2Cl_2. After evaporation to dryness, the CH_2Cl_2 crude extract was suspended in aqueous 5% HCl, then extracted with CH_2Cl_2. The crude alkaloid extract (29.5 g) obtained after solvent removal under reduced pressure was purified by repeated open column chromatography, eluted with a gradient of CH_2Cl_2/MeOH to afford myrobotinol (**1**, 20 mg).

Myrobotinol (1): solid, mp 225−226 °C (*n*-hexane/Et_2O); $[\alpha]^{20}_D$ +36.4 (*c* 0.4, MeOH); IR (KBr) ν_{max} (cm^{-1}) 3386, 2932, 2866, 1652, 1447, 1407, 1380, 1137, 1117, 1099, 1038, 1016, 993, 955, 921, 852, 827, 721, 599; ESI-MS (TOF), *m/z* 333.2538 $[M + H]^+$ (calcd.333.2542 for $C_{20}H_{33}N_2O_2$); ESI-MSMS (TOF), on $[M + H]^+$ ion, *m/z* 333, 290, 198, 196, 178, 168, 166, 150, 148, 124, 105, 91.

(*R*)-MTPA-Myrobotinol Ester (2). (*R*)-MTPA (10 mg, 0.43 mmol) was treated with $SOCl_2$ and a small amount of NaCl at rt for 48 h. Excess $SOCl_2$ was removed under diminished pressure, then the crude was co-evaporated with toluene to complete removal of $SOCl_2$. The remaining crude was dissolved in dry $CHCl_3$ (0.3 mL) and treated with myrobotinol (**1**, 3 mg, 0.009 mmol) in 0.1 mL of dry $CHCl_3$, a drop of pyridine was added, and the solution was stirred for 24 h. The volatile layer was removed under diminished pressure and the crude was purified by preparative TLC (CH_2Cl_2/MeOH 95/5) to afford **2** (3.5 mg, 75%). Colorless oil, $[\alpha]^{20}_D$ +36.4 (*c* 0.3, MeOH); ESI-MS (TOF), *m/z* 549.2958 $[M + H]^+$ (calcd. 549.2942 for $C_{30}H_{40}F_3N_2O_4$); ESI-MSMS (TOF), on $[M + H]^+$ ion, *m/z* 549 $[M + H]^+$, 506, 412, 382, 315, 272, 178, 150, 124; ^1H (400.13 MHz, $CDCl_3$, 298 K) 7.49 (m, 2H, H-5′ and H-9′), 7.38, (m, 1H, H-7′), 7.37 (m, 2H, H-6′ and H-8′), 5.13 (m, 1H, H-16), 4.20 (dd, 9.6 and 2.4 Hz, 1H, H-21), 4.12 (d, 3.3 Hz, 1H, H-11), 4.01 (dd, 10.8 and 4.5 Hz, 1H, H-13_{eq}), 3.5 (s, 3H, OMe-10′), 3.26 (dd, 10.8 and 10.8 Hz, 1H, H-13_{ax}), 3.11 (dd, 11.8 and 4.7 Hz, 1H, H-10), 2.74 (m, 1H, H-2_{eq}), 2.72 (dd, 11.4 and 4.6 Hz, 1H, H-23), 2.64 (m, 1H, H-2_{ax}), 2.28 (m, 1H, H-14), 2.23 (m, 1H, H-9), 1.99 (m, 1H, H-18), 1.93 (m, 1H, H-5), 1.91 (m, 1H, H-17_{eq}), 1.84 (m, 1H, H-15_{eq}), 1.73 (m, 1H, H-3_{eq}), 1.69 (m, 2H, CH_2-20), 1.59 (m, 1H, H-17_{ax}), 1.57 (m, 2H, CH_2-19), 1.53 (m, 1H, H-4_{ax}), 1.50 (m, 3H, H-3_{ax} and CH_2-6), 1.42 (m, 1H, H-8_{eq}), 1.38 (m, 2H, CH_2-7), 1.33 (m, 1H, H-8_{ax}), 1.27 (m,1H, H-4_{eq}), 1.01 (ddd, 12.0, 10.6 and 10.5 Hz, 1H, H-15_{ax}); ^{13}C (75.47 MHz, $CDCl_3$, 298 K) 165.8 (C-1′), 132.3 (C-4′), 129.6 (C-7′), 128.4 (C-6′ and C-8′), 127.3 (C-5′ and C-9′), 91.9 (C-11), 84.9 (C-2′), 72.8 (C-13), 71.5 (C-16), 68.8 (C-21), 64.2 (C-23), 57.4 (C-10), 55.3 (OMe-10′), 38.2 (C-2), 36.0 (C-18), 35.6 (C-17), 35.1 (C-5), 32.9 (C-15), 31.4 (C-6), 30.7 (C-9), 30.1 (C-20), 27.5 (C-8), 26.6 (C-14), 26.2 (C-3), 25.2 (C-19), 24.2 (C-4), 20.2 (C-7).

(*S*)-MTPA-Myrobotinol Ester (3). According to the above procedure, **3** (2.2 mg, 33% yield) was obtained from myrobotinol (4 mg) and (*S*)-MTPA (10 mg). Colorless oil, $[\alpha]^{20}_D$ −5 (*c* 0.25, MeOH); ESI-MS (TOF), *m/z* 549.2963 $[M + H]^+$ (calcd 549.2942 for $C_{30}H_{40}F_3N_2O_4$); ESI-MSMS (TOF), on $[M + H]^+$ ion, *m/z* 549 $[M + H]^+$, 506, 412, 315, 298, 285, 272, 190, 178, 150, 124; ^1H (400.13 MHz, $CDCl_3$, 298 K) 7.49 (m, 2H, H-5′ and H-9′), 7.38 (m, 1H, H-7′), 7.37 (m, 2H, H-6′ and H-8′), 5.13 (m, 1H, H-16), 4.21 (m, 1H, H-21), 4.11 (d, 3.1 Hz, 1H, H-11), 3.99 (dd, 10.9 and 4.5 Hz, 1H, H-13_{eq}), 3.51 (s, 3H, OMe-10′), 3.23 (dd, 10.9 and 10.9 Hz, 1H, H-13_{ax}), 3.11 (m, 1H, H-10), 2.77 (m, 1H, H-2_{eq}), 2.72 (m, 1H, H-23), 2.67, (m, 1H, H-2_{ax}), 2.26, (m, 1H, H-14), 2.22, (m, 1H, H-9), 1.99 (m, 2H, H-18 and H-17_{eq}), 1.93 (m, 1H, H-5), 1.75 (m, 1H, H-15_{eq}), 1.73 (m, 1H, H-3_{eq}), 1.69 (m, 3H, 17_{ax} and CH_2-20), 1.68 (m, 1H, H-19_{ax}), 1.58 (m, 1H, H-19_{eq}), 1.53 (m, 1H, H-4_{ax}), 1.50 (m, 3H, H-3_{ax} and CH_2-6), 1.42 (m, 1H, H-8_{eq}), 1.38 (m, 2H, CH_2-7), 1.33 (m, 1H, H-8_{ax}), 1.27 (m, 1H, H-4_{eq}), 0.90 (ddd, 12.0, 11.8 and 8.8 Hz, 1H, H-15_{ax}); ^{13}C (75.47 MHz, $CDCl_3$, 298 K) 165.8 (C-1′), 132.3 (C-4′), 129.6 (C-7′), 128.4 (C-6′ and C-8′), 127.2 (C-5′ and C-9′), 91.8 (C-11), 84.5 (C-2′), 72.3 (C-13), 71.5 (C-16), 68.8 (C-21), 64.5 (C-23), 57.4 (C-10), 55.3 (OMe-10′), 38.1 (C-2), 36.0 (C-18), 35.9 (C-17), 35.1 (C-5), 32.6 (C-15), 31.3 (C-6), 30.7 (C-9), 30.0 (C-20), 27.5 (C-8), 26.5 (C-14), 26.1 (C-3), 25.2 (C-19), 24.2 (C-4), 20.1 (C-7).

Acknowledgment. The authors thank Mr. A. Gramain and Mr. D. C. Dao (Institute of Chemistry−VAST, Vietnam) for plant collection and its botanical determination, Dr. A. Blond and Mr. Lionel Dubost (MNHN, France) for recording 2D NMR spectra and ESI-MS measurement, respectively, and Prof. P. Grellier (MNHN, France) for antiplasmodial assay. The CNRS is gratefully acknowledged for doctoral fellowship support (V.C.P.).

Supporting Information Available: NMR and MS spectra of myrobotinol (**1**). This material is available free of charge via the Internet at http://pubs.acs.org.

JO7017203